Gas exchange calculation may estimate changes in pulmonary blood flow during veno-arterial extracorporeal membrane oxygenation in a porcine model.

Kaspar Felix Bachmann MD[1,2], Matthias Haenggi MD[2], Stephan M Jakob MD PhD[2], Jukka Takala MD PhD[2], Luciano Gattinoni MD PhD[3], David Berger MD[2]

1 Department of Anesthesiology & Pain Medicine, Inselspital, Bern University Hospital, University of Bern, Bern, Switzerland

2 Department of Intensive Care Medicine, Inselspital, Bern University Hospital, University of Bern, Bern, Switzerland

3 Department of Anesthesiology, Emergency and Intensive Care Medicine, University of Göttingen, Göttingen, Germany.

Corresponding Author:
Kaspar Felix Bachmann, MD
Department of Anaesthesiology & Pain Medicine and Department of Intensive Care Medicine, Inselspital, Bern University Hospital, University of Bern, Bern, Switzerland
kaspar.bachmann@insel.ch
+41 31 621 21 11

Authors contribution: KFB, DB: conception and design, experimentation, data analysis, draft of the manuscript. MH: experimentation, critical review of the manuscript SJM, JT: Critical review of the manuscript. LG conception, critical review of the manuscript. All authors read and agreed to the final version of the manuscript.

Prior Presentations: none

Word and Element Counts: Abstract 250; Introduction: 255, Discussion: 1059. Number of figures: 5. Number of Tables: 2. Number of Appendices: 1.

Running Head: Calculating cardiac output during V-A ECMO via gas exchange.

Summary Statement: Weaning of veno-arterial ECMO remains a challenge despite its growing use a rescue therapy. We show in this proof of concept study that blood flow estimation from exhaled CO_2 is feasible with simple, non-invasive measurements and acceptable accuracy.

Conflicts of Interests/Financial Disclosures: The Department of Intensive Care Medicine, University Hospital Bern, has, or has had in the past, research contracts with Orion Corporation, Abbott Nutrition International, B. Braun Medical AG, CSEM SA, Edwards Lifesciences Services GmbH, Kenta Biotech Ltd, Maquet Critical Care AB, Omnicare Clinical Research AG and research & development/consulting contracts with Edwards Lifesciences SA, Maquet Critical Care AB, and Nestlé. The money was paid into a departmental fund; no author received personal financial gain. Authors Bachmann, Berger and Gattinoni filed a patent for the method described.

The Department of Intensive Care Medicine has received unrestricted educational grants from the following organizations for organizing a quarterly postgraduate educational symposium, the Berner Forum for Intensive Care (until 2015): Fresenius Kabi, GSK, MSD, Lilly, Baxter, Astellas, AstraZeneca, B | Braun, CSL Behring, Maquet, Novartis, Covidien, Nycomed, Pierre Fabre Pharma AG (formerly known as RobaPharm), Pfizer, Orion Pharma, Bard Medica S.A., Abbott AG, Anandic Medical Systems.

The Department of Intensive Care Medicine has received unrestricted educational grants from the following organizations for organizing bi-annual postgraduate courses in the fields of critical care ultrasound, management of ECMO and mechanical ventilation: Pierre Fabre Pharma AG (formerly known as RobaPharm), Pfizer AG, Bard Medica S.A., Abbott AG, Anandic Medical Systems, PanGas AG Healthcare, Orion Pharma, Bracco, Edwards Lifesciences AG, Hamilton Medical AG, Fresenius Kabi (Schweiz) AG, Getinge Group Maquet AG, Dräger Schweiz AG, Teleflex Medical GmbH.

Abstract

Background: Veno-arterial extracorporeal membrane oxygenation (V-A ECMO) is used as rescue for severe cardiopulmonary failure. We tested whether the ratio of CO_2 elimination at the lung and the V-A ECMO ($\dot{V}CO_{2ECMO}/VCO_{2Lung}$) would reflect the ratio of respective blood flows and could be used to estimate changes in pulmonary blood flow (Q_{LUNG}), i. e. native cardiac output.

Methods: Four healthy pigs were centrally cannulated for V-A ECMO. We measured blood flows with an ultrasonic flow probe. $\dot{V}CO_{2ECMO}$ and $\dot{V}CO_{2Lung}$ were calculated from sidestream capnographs under constant pulmonary ventilation during V-A ECMO weaning with changing sweep gas and/or V-A ECMO blood flow. If ventilation/perfusion (V/Q) ratio of V-A ECMO was not one, the $\dot{V}CO_{2ECMO}$ was normalized to V/Q=1 ($\dot{V}CO_{2ECMONORM}$). Changes in pulmonary blood flow were calculated using the relationship between changes in CO_2 elimination and V-A ECMO blood flow.

Results: Q_{ECMO} correlated strongly with $\dot{V}CO_{2ECMONORM}$ (r2 0.95 – 0.99). Q_{LUNG} correlated well with $\dot{V}CO_{2LUNG}$ (r2 0.65 – 0.89, p<=0.002). Absolute Q_{Lung} could not be calculated in a non-steady state. Calculated pulmonary blood flow changes had a bias of 76 (-266 to 418) ml/min and correlated with measured Q_{LUNG} (r2 0.974 – 1.000, p = 0.1 to 0.006) for cumulative ECMO flow reductions.

Conclusions: $\dot{V}CO_2$ of the lung correlated strongly with pulmonary blood flow. Our model could predict pulmonary blood flow changes within clinically acceptable margins of error. The prediction is made possible with a normalization to a V/Q of 1 for ECMO. This approach depends on measurements readily available and may allow immediate assessment of the cardiac output response.

Introduction

Extracorporeal membrane oxygenation (ECMO) is increasingly used as rescue therapy for severe cardiopulmonary failure (2). In veno-arterial (V-A) ECMO treatment, the native heart and lung work in parallel with the extracorporeal circuit and the assessment of native cardiac output (i. e. blood flow through the lungs (Q_{LUNG})) is difficult. The ongoing unloading of the right ventricle even at low V-A ECMO blood flow (Q_{ECMO}) makes assessment of cardiac function during V-A ECMO treatment challenging. Monitoring of the cardiac function and the evolution of native cardiac output during V-A ECMO treatment are not well standardized. Echocardiography is often used, but requires specific knowledge (1) and routine echocardiographic parameters may not be useful in the context because of altered circulatory physiology and changing cardiac loading conditions (12). Monitoring of the evolution of native cardiac output based on simple, non-invasive and readily available measurements would therefore be helpful in clinical practice, particularly during weaning, since early weaning success is associated with a favorable prognosis (9).

Gas exchange during V-A ECMO should reflect the combined effect of ventilation and perfusion of the native lung and those of the V-A ECMO circuit (21). We hypothesize that during V-A ECMO weaning the ratio between changes in $\dot{V}CO_{2ECMO}$ and $\dot{V}CO_{2Lung}$ is the same as the ratio between changes in the respective flows (Q_{ECMO} and Q_{LUNG}). We tested this hypothesis in this preliminary, hypothesis generating study by measuring the elimination of CO_2 over the native lung and the V-A ECMO and the respective blood flows, and compared the calculated flow changes with those directly measured from the pulmonary artery and V-A ECMO circuit.

Methods

Animal Care, surgery and anesthesia

This study was performed as a preliminary, independent sub-study of a yet unpublished project evaluating regional abdominal circulation during V-A ECMO and systemic inflammation, where measurements were done before the main study protocol was started. The study complied with the Guide for the Care and Use of Laboratory Animals (National Academy of Sciences, 1996) and Swiss National Guidelines and was approved, including an amendment for this sub-study, by the Commission of Animal Experimentation of Canton Bern, Switzerland (BE119/17).

We studied a convenience sample of four animals (2 male and female each, 51.5 ± 1.3 kg) before the main study protocol was started. The pigs fasted for 12h with free access to water. After anesthesia induction with intravenous midazolam and atropine and oral intubation, anesthesia was maintained with propofol and fentanyl and the depth was controlled by repeatedly testing the response to nose pinch in additional to bispectral index target < 60 (BIS™ Quatro, Covidien, Mansfield, MA). Additional injections of fentanyl (50 µg) or midazolam (5 mg) were given as needed. Muscle relaxation was induced with rocuronium (0.5 mg/kg). Mechanical ventilation (volume control mode, PEEP 5 cmH_2O, FiO2 0.3) was initiated with a tidal volume of 7 ml/kg and a respiratory rate aiming at an end-tidal pCO_2 of 45 mmHg. A 5 French introducer sheath was placed in the right carotid artery for arterial blood pressure measurement and arterial blood gas sampling. Two three-lumen central venous lines were placed in the right and left jugular vein for right atrial pressure measurement and continuous administration of sedatives and vasopressors. V-A ECMO with right atrial-aortic cannulation and a left atrial vent (Maquet Cardiohelp, Quadrox MECC oxygenator, Rastatt, Germany and Medtronic cannula and vent, Minneapolis, MN) were installed via a sternotomy and a bolus of 2.500 IE unfractioned heparin was given. An appropriately sized ultrasonic flow probe was placed on the pulmonary artery (16 or 18 mm internal diameter, Transonic PAU series, Ithaca, USA). During surgery, fluid was supplemented with Ringer's lactate at an initial rate of 5 ml · kg-1 · min-1 and increased to 10ml · kg-1 · min-1. Any visible blood loss was replaced by hydroxyethyl starch (HES; 6% Voluven; Fresenius Kabi, Bad Homburg, Germany), and V-A ECMO pump speed adjusted to achieve a mixed or central venous saturation > 50%.

Measurements and data recording

Pulmonary blood flow, i. e. cardiac output (Q_{LUNG}) and V-A ECMO blood flow (Q_{ECMO}) were measured on the pulmonary artery main trunk and arterial ECMO tubing (Transonic PAU series, Ithaca, USA). Pulmonary end-tidal pCO_2 ($etCO_{2LUNG}$) and pCO_2 at the membrane lung ($peCO_{2ECMO}$) were measured with a sidestream capnograph (GE Medical, Module E-COVX with automated correction to BTPS conditions). The carbon dioxide production ($\dot{V}CO_2$) was calculated individually for native and membrane lungs from the tidal pCO_2 tracing as described below. We recorded sweep gas flow (V_{ECMO}) manually. Arterial blood gases were taken before and after the study period. Pulmonary ventilation (V_{LUNG}) was kept constant. In the first animal, ventilator settings were kept identical to those before V-A ECMO (tidal volume (VT) 0.465 L, 12 breaths/min), whereas in the subsequent animals, V_{LUNG} was reduced to 2 liters/minute (VT 0.25, 8 breaths /min) as V-A ECMO was started and kept constant thereafter. In all animals 5 cmH_2O PEEP and volume control mode was used (Servo-i, Maquet, Solna, Sweden). The fraction of inspired oxygen was set at 0.30. Measurements were performed in healthy animals, 30 minutes after surgery was completed. Eventually, the pigs were euthanized by injection of 40 mmol of potassium chloride and V-A ECMO stopped in deep anesthesia. Data were recorded using Labview™ (National Instruments Corp., Austin, TX,) for offline analysis with Soleasy (Alea Solutions, Zürich, Switzerland) and Matlab R2019a (MathWorks, Natick, Massachusetts, USA).

Experimental protocol

The experiment consisted of 3 phases with varying sweep gas/blood flow ratios (i. e. the "(V/Q-ratio" of the membrane lung) in order to determine how the sweep gas/blood flow relationship at the V-A ECMO influences extracorporeal CO_2 elimination (VCO_{2ECMO}). First, we reduced Q_{ECMO} and $\dot{V}_{ECMO}$ in parallel (stable V/Q = 1, phase: "*reduction of* V*&Q*", $rV\&Q_{ECMO}$). Then we lowered V_{ECMO} with a constant Q_{ECMO} (V/Q towards shunt, phase: "*reduction of* V", rV_{ECMO}). Finally, we tested an V-A ECMO weaning trial, where Q_{ECMO} was reduced but V_{ECMO} was kept constant (V/Q towards dead space, phase: "*reduction of Q*", rQ_{ECMO}).

Q_{ECMO} and V_{ECMO} were set at 4 L/min each at baseline and afterward reduced – depending on the respective phase - to 75%, 50%, and 25% of baseline with an interval of one minute for each condition (Figure 1). The left atrial vent was clamped during these procedures and the stepwise reduction of blood flow was not supported by vasopressors or inotropes.

Calculation of $\dot{V}CO_2$ for V-A ECMO

Expiratory concentration of CO_2 at the V-A ECMO exhaust was calculated from the expiratory partial pressure of CO_2 at the V-A ECMO exhaust, and used to calculate $\dot{V}CO_2$ (16, 23), using actual barometric pressures (on average 722mmHg). The experiments were performed at 540 meters above sea level.

$$(1)\ \dot{V}CO_{2ECMO} = \mathrm{FeCO_2} * V_{ECMO} = \frac{peCO_{2ECMO} * V_{ECMO}}{barometric\ pressure}$$

Calculation of VCO2 for the lung

Mean pulmonary expired carbon dioxide ($pECO_2$) was calculated by averaging the end-tidal carbon dioxide ($petCO_2$) curve over the respiratory cycle with correction for the inspiratory to expiratory (I:E) ratio:

$$(2)\ pECO_2 = pECO_2 * \frac{(I+E)}{E}$$

This was verified by integration of the expiratory pCO_2 curve, which delivers the same result. We then calculate $\dot{V}CO_{2LUNG}$:

$$(3)\ \dot{V}CO_{2LUNG} = FeCO_2 * V_{LUNG} = \frac{pECO_2 * V_{LUNG}}{barometric\ pressure}$$

Blood flow calculations

Figure 2 depicts the situation during V-A ECMO schematically. We define the following relationships, whereby Q is flow and Δv-aCO_2 is the inflow-outflow difference in blood CO_2 content in a given segment ($\Delta_{v-ao}CO_2$ is the difference between venous and aortal CO_2 content, $\Delta_{v-LA}CO_2$ is the difference between venous and left atrial CO_2 content, $\Delta_{v-pm}CO_2$ is the difference between venous and post membrane CO_2 content):

$$(4)\ Q_{total} = Q_{LUNG} + Q_{ECMO}$$
$$(5)\ \dot{V}CO_{2_{total}} = \dot{V}CO_{2_{LUNG}} + \dot{V}CO_{2_{ECMO}}$$
$$(6)\ \dot{V}CO_{2_{LUNG}}\ and\ \dot{V}CO_{2_{ECMO}} = Q * \Delta_{v-a}CO_2;\ \dot{V}CO_{2_{total}} = Q_{total} * \Delta_{ao-v}CO_2$$

We then implement equation (4) and (6) into equation (5):

$$(7)\ Q_{total} * \Delta_{ao-v}CO_2 = Q_{LUNG} * \Delta_{v-LA}CO_2 + Q_{ECMO} * \Delta_{v-pm}CO_2$$

We now solve equation (7) for Q_{LUNG}:

$$Q_{total} * \Delta_{ao-v}CO_2 = Q_{LUNG} * \Delta_{v-LA}CO_2 + Q_{ECMO} * \Delta_{v-pm}CO_2$$

$$(Q_{LUNG} + Q_{ECMO}) * \Delta_{ao-v}CO_2 = Q_{LUNG} * \Delta_{v-LA}CO_2 + Q_{ECMO} * \Delta_{v-pm}CO_2$$

$$Q_{LUNG} * (\Delta_{ao-v}CO_2 - \Delta_{v-LA}CO_2) = Q_{ECMO} * (\Delta_{v-pm}CO_2 - \Delta_{ao-v}CO_2)$$

$$(8)\ Q_{LUNG} = Q_{ECMO} * \frac{(\Delta_{v-pm}CO_2 - \Delta_{ao-v}CO_2)}{(\Delta_{ao-v}CO_2 - \Delta_{v-LA}CO_2)}$$

As we aim to calculate Q_{LUNG} with expired gas phase measurements only rather than calculating blood gas content from multiple blood gas samples, we modify equation (8) with the following assumptions. As carbon dioxide production and carbon dioxide elimination are mathematical opposites, we use the absolute value function, thus eliminating negative values.

$$(9)\ \Delta_{ao-v}CO_2 \sim |\dot{V}CO_{2_{total}}|$$
$$(10)\ \Delta_{v-LA}CO_2 \sim |\dot{V}CO_{2_{LUNG}}|$$
$$(11)\ \Delta_{v-pm}CO_2 \sim |\dot{V}CO_{2_{ECMO}}|$$

We now implement these equations (9-11) into equation (8).

$$(12)\ Q_{LUNG} = Q_{ECMO} * \frac{(|\dot{V}CO_{2_{ECMO}}| - |\dot{V}CO_{2_{total}}|)}{(|\dot{V}CO_{2_{total}}| - |\dot{V}CO_{2_{LUNG}}|)}$$

Equation (5) simplifies (12) to:

$$(13)\ Q_{LUNG} = Q_{ECMO} * \frac{|\dot{V}CO_{2_{LUNG}}|}{|\dot{V}CO_{2_{ECMO}}|}$$

There is a fixed relationship of Q_{LUNG} and Q_{ECMO} with the respective eliminated CO_2. This expresses our hypothesis that the ratio between the differences in $\dot{V}CO_{2ECMO}$ and $\dot{V}CO_{2Lung}$ is the same as the ratio between the differences in the respective flows (Q_{ECMO} and Q_{LUNG}). In our experimental setup, we cannot expect to reach a steady state as step changes were set at 1 minute. Therefore, we calculate pulmonary blood flow using the differences in $\dot{V}CO_2$ and Q_{ECMO} during V-A ECMO weaning rather than applying it to steady state conditions.

$$(14)\Delta Q_{LUNG} = \Delta Q_{ECMO} * \frac{\Delta\dot{V}CO_{2_{LUNG}}}{\Delta\dot{V}CO_{2_{ECMO}}}$$

Normalization of uneven V/Q ratios at the V-A ECMO

During phase *"rV&Q_{ECMO}"* with a constant V/Q_{ECMO} of 1, we expect relationship (14) to work. However, $\Delta \dot{V}CO_{2ECMO}$ is influenced by V_{ECMO} and Q_{ECMO}. Q_{ECMO} determines the amount of CO_2 transported towards the membrane lung, while V_{ECMO} determines the amount of CO_2 eliminated over the membrane lung with a major impact on $\Delta \dot{V}CO_{2ECMO}$ (10, 13, 17). $\Delta \dot{V}CO_{2ECMO}$ does therefore not necessarily represent ΔQ_{ECMO}, when V/Q_{ECMO} differs from 1. During the phase *" rQ_{ECMO}"*, $\dot{V}CO_2$ may decouple from Q_{ECMO}. Accordingly, the ratio $\Delta \dot{V}CO_{2ECMO}/\Delta \dot{V}CO_{2LUNG}$ is affected by V_{ECMO} despite unchanged blood flows.

In order to correct for uneven V/Q, we normalized $\Delta \dot{V}CO_{2ECMO}$ into a new variable, $\Delta \dot{V}CO_{2ECMONORM}$, only dependent on Q_{ECMO} and independent of V_{ECMO} with formula (15). The correction factor f is expressed in formula (16).

$$(15)\ \Delta\dot{V}CO_{2_{ECMONORM}} = \Delta\dot{V}CO_{2_{ECMO}} * f$$

$$(16)\ f(V,Q) = \frac{Q * \left(\frac{V}{Q} + c\right)}{V * (1 + c)}$$

A formal deduction of this normalization is found in the Appendix (See Appendix A, Normalization function).

Statistical Analysis

For statistical, mathematical and graphical analysis, we used Matlab R2019a (MathWorks, Natick, Massachusetts, USA) including an extension pack under a creative commons license for the creation of Bland-Altman plots (15). Data are presented either individually or as range. Correlation coefficients were calculated using Pearson's square (r^2). Agreement between methods (calculated and measured Q_{LUNG}) was assessed with Bland-Altman analysis.

Results

Baseline

At baseline V_{ECMO} and Q_{ECMO} of 4 L/min, $\dot{V}CO_{2ECMO}$ was between 202 and 243 ml/min, while $\dot{V}CO_{2LUNG}$ was between 13 and 193 ml/min, corresponding to a measured Q_{LUNG} of 10 to 964 mL/min and representing a normal $\dot{V}CO_2$ production for swine (6) (Step 1 for V, Q and VQ in Table 1).

Measurements at the V-A ECMO

Per protocol, Q_{ECMO} remained unchanged from baseline during phase *"rV_{ECMO}"* (98 – 100 % of baseline or 3989 - 4186 l/min) and was reduced to a quarter of baseline in phase "*R V/Q*" (641 - 1178 ml/min, 16 – 29 % of baseline). In phase "*rQ_{ECMO}"*, Q_{ECMO} was reduced to approximately a quarter in all animals except animal 3 due to hemodynamic instability (25.4 – 49.5% of baseline or 1048 -1994 ml/min) (Table 1).

The normalization function was calculated by fitting our data points into formula (16) and retrieving the constant c = 1.157 (r^2 = 0.995, p < 0.001). $\dot{V}CO_{2ECMONORM}$ correlated highly with Q_{ECMO} and the normalization improves correlation significantly (Figure 3A and B). In phase "*rV_{ECMO}"*, reducing V_{ECMO} without any change in Q_{ECMO}, $\dot{V}CO_{2ECMONORM}$ was 194 – 249 ml/min or 93.3 – 100.1 % of baseline. Without normalization, $\dot{V}CO_{2ECMO}$ decoupled from Q_{ECMO} with a decrease from 205 – 246 ml/min to 73 – 96 ml/min in this phase (Table 1, Figure 4B). $\dot{V}CO_{2ECMO}$ values for phase: "*$rV\&Q_{ECMO}$*" dropped to roughly a quarter from baseline (64 - 74 ml/min, 25 – 33% of baseline) in parallel with reduced Q_{ECMO}. During phase: "*rQ_{ECMO}*", $\dot{V}CO_{2ECMONORM}$ was 84 – 156 ml/min or 38 – 58 % of baseline.

Measurements at the lung

During unchanged Q_{ECMO} (phase "*rV_{ECMO}*") Q_{Lung} remained close to baseline (2 - 980 ml/min) and did not change much within one animal and $\dot{V}CO_2$ stayed constant, accordingly.

During reduction of Q_{ECMO} in phase "*$rV\&Q_{ECMO}$*" and phase "*rQ_{ECMO}"*, Q_{LUNG} increased from its low baseline values to 928 - 1550 ml/min, and 328 - 1914 ml/min, respectively (Table 1). $\dot{V}CO_{2LUNG}$ followed the changes in Q_{LUNG} to 74 – 232 ml/min (rise of 28 – 57 ml/min from baseline, with stepwise increases in every animal) for *"$rV\&Q_{ECMO}$"* and 39 – 233 ml/min for *"rQ_{ECMO}"* (rise of 18 – 45 ml/min from baseline), and remained steady at full Q_{ECMO} (phase "*rV_{ECMO}*", 21 – 188 ml/min,

235 change of 7 – 8 ml/min from baseline) (Table 2). Q_{LUNG} and $\dot{V}CO_{2LUNG}$ showed a high correlation
236 (Figure 4).

237 Calculation of Q_{LUNG}

238 The calculation of pulmonary blood flow from absolute $\dot{V}CO_2$ values is imprecise and leads to a
239 consistent overestimation (Table 1). This overestimation increases with increasing V/Q ratio at
240 the lung, which is shown in animal 1, where we had increased ventilation compared to the other
241 animals. In phase "rV_{ECMO}", we observe no change in measured Q_{LUNG} as well as calculated
242 changes in Q_{LUNG} , When differences between the short stepwise flow reductions are considered
243 (Table 2), correlations are reestablished (Figure 5B) and the respective Bland Altman Plot
244 (Figure 5A) shows a small bias with acceptable limits of agreement. True blood flow changes are
245 underestimated since bias is positive. Bias stays constant over the measured range (R^2 = -0.16,
246 p = 0.5). When the phase "rV_{ECMO}" is excluded due to no expected change in blood flow, out of
247 23 blood flow change calculations, an opposite direction of the flow change is calculated in four
248 instances. In all of these instances, the value of the change is below the least significant change,
249 which is 113 ml/min. When the entire reduction steps are summarized (Table 2 and Figure 5C),
250 the relationship becomes overt.

Discussion

We show in a preliminary analysis that measurements of $\dot{V}CO_2$ at both lung and V-A ECMO are possible with simple side-stream technology. Our model for the estimation of changes in Q_{LUNG} predicts the directional change of pulmonary blood flow, i. e. cardiac output with acceptable accuracy in this small sample size (3). The measurements needed for our calculations (Q_{ECMO}, V_{ECMO}, V_{LUNG}, $peCO_{2ECMO}$, $etCO_{2LUNG}$) are easily performed with use of standard side-stream capnographs, all of which are readily available in an ICU setting or an operating theater and require no specific training.

As expected from the ventilation-perfusion concept and the gas content equations in figure 2 (14), we found that a decrease in Q_{ECMO} and the consecutive increase in Q_{LUNG} leads to a respective change in $\dot{V}CO_{2LUNG}$ and $\dot{V}CO_{2ECMONORM}$. A closer look at formula (8) as the background of our hypothesis shows an adaptation of the classic Berggren-shunt equation (11). This seems intuitive, as the V-A ECMO is in concept an anatomical right-to-left shunt, where the ability to ventilate and oxygenate the shunted blood will clearly affect its functional influence (Figure 2). Changing the sweep gas/blood flow ratio on the ECMO will vary the function of this anatomical shunt from true shunt (V_{ECMO} = 0 at any Q_{ECMO}) to dead space (Q_{ECMO} = 0 at any $\dot{V}_{ECMO}$). $\dot{V}CO_{2ECMO}$ only represents the shunt correctly, as long as sweep gas/blood flow on the V-A ECMO are kept at a ratio of 1 (in phase "*$rV\&Q_{ECMO}$*"). For sweep gas/blood flow ratios differing from one, sweep gas flow (V_{ECMO}) will drastically change the amount of the eliminated CO_2 (10, 17) independently of blood flow - a known phenomenon in states of shock or multiorgan failure (13). We could simulate this in the derivation of our normalization procedure (See Appendix A, Appendix figures 2 and 3) and reproduce it in the experiment during the steps "*rV_{ECMO}*" (Table 1).

The normalization of $\dot{V}CO_{2ECMO}$ reestablishes a sweep gas/blood flow ratio of 1, and therefore restores the correlation between $\dot{V}CO_{2ECMONORM}$ and Q_{ECMO}. This newly calculated $\dot{V}CO_{2ECMONORM}$ now is only dependent on blood flow and independent from ventilation and thus eliminates the influence of V/Q_{ECMO} mismatch on blood flow calculations. We used our data to calculate the constant c with a curve fitting function, in order to stay independent from blood gas measurements, although individual calculations would be possible to from pre-membrane pH. We see the high goodness of fit of this normalization procedure as an indirect proof of the normalization function (See Appendix A, Appendix figure 6). During V-A ECMO weaning with a sweep gas/blood flow ratio of 1, it seems of little practical importance. Normalization might be

particularly helpful to wean a low blood flow system with the primary intention to eliminate CO2, where the effect of increased ventilation is most relevant (5). (See Appendix A, Appendix figure 3). Whether this might be applicable to a veno-venous configuration would need to be investigated. In a veno-arterial configuration, normalization might allow accurate estimations of post-membrane CO_2 pressures in blood, enabling a continuous gaseous oxygenator measurement to derive blood gas tensions (See Appendix A, figure 2).

A high V/Q_{Lung} ratio will significantly increase the overall amount of CO_2 eliminated and thus lead to an overestimation of pulmonary blood flow, while a reduction in V_{ECMO} will lead to a decrease in eliminated CO_2 and thus to a rise in venous CO_2 content. This in turn increases $\dot{V}CO_{2LUNG,}$ to achieve a new steady state. However, as the V-A ECMO and the lung both drain venous blood from the right atrium, $\dot{V}CO_{2ECMO}$ should increase simultaneously with the new steady state in order to fulfill formula (5). Our short measurement periods did preclude a steady state for CO_2 elimination. Calculations of total blood flow for any given moment may therefore be impossible, because the lack of a steady state does not allow for sufficient accuracy. As we calculated Q_{LUNG} through a deliberate step change in $\dot{V}CO_2$, a steady state is not necessary, as there is no need for an absolute reference point. This also allows the calculations for different settings of V_{LUNG} (as shown with animal 1), as long as V_{LUNG} remains constant.

The ratio of ventilation to perfusion in the lung will vary with hypoxic vasoconstriction, shunt, alveolar collapse and dead space. Our $\dot{V}CO_{2LUNG}$ – estimated from end-tidal pCO_2 in healthy lungs - showed an acceptable relationship with Q_{LUNG}, but stable minute ventilation on the lung was mandatory. As Q_{LUNG} is the quantity to be calculated, a normalization procedure is not possible. As $\dot{V}CO_{2LUNG}$ can only represent blood flow that participates in gas exchange, shunt due to supine positioning of the animals could explain the bias of underestimation of changes in pulmonary blood flow with our method.

There are several possible limitations to our method: Firstly, a V/Q_{LUNG} mismatch (e.g. high shunt and/or high dead space) might result in a decrease of Q_{Lung} – $\dot{V}CO_{2Lung}$ correlation and might thus increase the bias significantly. Secondly, we did not document every V-A ECMO flow change with blood gas samples, because our aim was to calculate Q_{LUNG} using gaseous measurements. Nevertheless, a meticulous documentation of blood gas status would strengthen our hypothesis and allow for alternative calculations of gas content and direct calculations of the normalization function. Thirdly, $\dot{V}CO_2$ was calculated using side-stream capnography, which are of limited

accuracy. Signal shifts in the pCO_2-time tracing may introduce an error here. We did not rely on a breath-by-breath measurement, but averaged values over one minute may help to minimize this possible influence. Mainstream calorimetric modules are available and used in assessing cardiac output, alveolar and dead space ventilation (7, 18-20). Mainstream capnography at the V-A ECMO gas outlet is feasible and may deliver accurate results for $\dot{V}O_2$ and $\dot{V}CO_2$ (4, 22). This might improve our results and overall accuracy compared to our calculations from side-stream end-tidal carbon dioxide. Fourthly, this study was conducted in a small, clearly preliminary set of healthy animals and without any cardiovascular support.

The large scatter in pulmonary flow reflects the individual variability of native cardiac output during V-A ECMO treatment. In conclusion, we show that measurement of $\dot{V}CO_2$ at the V-A ECMO are easily performed. A normalization procedure allows estimation of $\dot{V}CO_2$ only dependent on blood flow without the influence of a V/Q mismatch. This in turn lays the basis of blood flow calculations using $\dot{V}CO_2$ values. Calculations of pulmonary blood flow using absolute values of carbon dioxide elimination are not possible in a non-steady state with our method. The concept can be derived from basic physiological equations. Whether our method may result in a clinically useful approach and support V-A ECMO weaning, where assessment of cardiac output may help to evaluate weanability, has to be further evaluated. These preliminary findings need further confirmation in a larger study, also investigating low and high V/Q states at the lung before exploring clinical applications.

References

1. **Cavarocchi NC, Pitcher HT, Yang Q, Karbowski P, Miessau J, Hastings HM, and Hirose H.** Weaning of extracorporeal membrane oxygenation using continuous hemodynamic transesophageal echocardiography. *The Journal of thoracic and cardiovascular surgery* 146: 1474-1479, 2013.

2. **Combes A, Brodie D, Chen Y-S, Fan E, Henriques JPS, Hodgson C, Lepper PM, Leprince P, Maekawa K, Muller T, Nuding S, Ouweneel DM, Roch A, Schmidt M, Takayama H, Vuylsteke A, Werdan K, and Papazian L.** The ICM research agenda on extracorporeal life support. *Intensive care medicine*, 2017.

3. **Critchley LA and Critchley JA.** A meta-analysis of studies using bias and precision statistics to compare cardiac output measurement techniques. *Journal of clinical monitoring and computing* 15: 85-91, 1999.

4. **De Waele E, van Zwam K, Mattens S, Staessens K, Diltoer M, Honore PM, Czapla J, Nijs J, La Meir M, Huyghens L, and Spapen H.** Measuring resting energy expenditure during extracorporeal membrane oxygenation: preliminary clinical experience with a proposed theoretical model. *Acta Anaesthesiol Scand* 59: 1296-1302, 2015.

5. **Duscio E, Cipulli F, Vasques F, Collino F, Rapetti F, Romitti F, Behnemann T, Niewenhuys J, Tonetti T, Pasticci I, Vassalli F, Reupke V, Moerer O, Quintel M, and Gattinoni L.** Extracorporeal CO2 Removal: The Minimally Invasive Approach, Theory, and Practice. *Crit Care Med* 47: 33-40, 2019.

6. **Hannon JP, Bossone CA, and Wade CE.** Normal physiological values for conscious pigs used in biomedical research. *Laboratory animal science* 40: 293-298, 1990.

7. **Jonson B.** Volumetric Capnography for Non-invasive Monitoring of ARDS. *American journal of respiratory and critical care medicine*, 2018.

8. **Keener JS, J.** Ventilation and Perfusion. In: *Mathematical Physiology: Systems Physiology* (Second Edition ed.), edited by Antman SM, J. Sirovich L. New York: Springer, 2009, p. 694-701.

9. **Lee SH, Chung CH, Lee JW, Jung SH, and Choo SJ.** Factors predicting early- and long-term survival in patients undergoing extracorporeal membrane oxygenation (ECMO). *Journal of cardiac surgery* 27: 255-263, 2012.

10. **Lehle K, Philipp A, Hiller KA, Zeman F, Buchwald D, Schmid C, Dornia C, Lunz D, Muller T, and Lubnow M.** Efficiency of gas transfer in venovenous extracorporeal membrane oxygenation: analysis of 317 cases with four different ECMO systems. *Intensive care medicine* 40: 1870-1877, 2014.

11. **Leigh JM, Tyrrell MF, and Strickland DA.** Simplified versions of the shunt and oxygen consumption equations. *Anesthesiology* 30: 468-470, 1969.

12. **Morimont P, Lambermont B, Guiot J, Tchana Sato V, Clotuche C, Goffoy J, and Defraigne JO.** Ejection Fraction May Not Reflect Contractility: Example in Veno-Arterial Extracorporeal Membrane Oxygenation for Heart Failure. *ASAIO journal (American Society for Artificial Internal Organs : 1992)* 64: e68-e71, 2018.

13. **Park M, Costa EL, Maciel AT, Silva DP, Friedrich N, Barbosa EV, Hirota AS, Schettino G, and Azevedo LC.** Determinants of oxygen and carbon dioxide transfer during extracorporeal membrane oxygenation in an experimental model of multiple organ dysfunction syndrome. *PloS one* 8: e54954, 2013.

14. **Radermacher P, Maggiore SM, and Mercat A.** Fifty Years of Research in ARDS. Gas Exchange in Acute Respiratory Distress Syndrome. *Am J Respir Crit Care Med* 196: 964-984, 2017.

15. **Rik.** BlandAltmanPlot. 2019.

16. **Scaravilli V, Kreyer S, Belenkiy S, Linden K, Zanella A, Li Y, Dubick MA, Cancio LC, Pesenti A, and Batchinsky AI.** Extracorporeal Carbon Dioxide Removal Enhanced by Lactic Acid Infusion in Spontaneously Breathing Conscious Sheep. *Anesthesiology* 124: 674-682, 2016.

17. **Sun L, Kaesler A, Fernando P, Thompson AJ, Toomasian JM, and Bartlett RH.** CO2 clearance by membrane lungs. *Perfusion* 33: 249-253, 2018.

18. **Tusman G, Groisman I, Maidana GA, Scandurra A, Arca JM, Bohm SH, and Suarez-Sipmann F.** The Sensitivity and Specificity of Pulmonary Carbon Dioxide Elimination for Noninvasive Assessment of Fluid Responsiveness. *Anesthesia and analgesia* 122: 1404-1411, 2016.

19. **Tusman G, Suarez-Sipmann F, Bohm SH, Borges JB, and Hedenstierna G.** Capnography reflects ventilation/perfusion distribution in a model of acute lung injury. *Acta Anaesthesiol Scand* 55: 597-606, 2011.

20. **Verscheure S, Massion PB, Verschuren F, Damas P, and Magder S.** Volumetric capnography: lessons from the past and current clinical applications. *Critical care* 20: 184, 2016.

21. **West JB.** Understanding pulmonary gas exchange: ventilation-perfusion relationships. *Journal of applied physiology (Bethesda, Md : 1985)* 97: 1603-1604, 2004.

22. **Wollersheim T, Frank S, Muller MC, Skrypnikov V, Carbon NM, Pickerodt PA, Spies C, Mai K, Spranger J, and Weber-Carstens S.** Measuring Energy Expenditure in extracorporeal lung support Patients (MEEP) - Protocol, feasibility and pilot trial. *Clinical nutrition* 37: 301-307, 2018.

23. **Zanella A, Mangili P, Giani M, Redaelli S, Scaravilli V, Castagna L, Sosio S, Pirrone F, Albertini M, Patroniti N, and Pesenti A.** Extracorporeal carbon dioxide removal through ventilation of acidified dialysate: an experimental study. *The Journal of heart and lung transplantation : the official publication of the International Society for Heart Transplantation* 33: 536-541, 2014.

Figure legends

Figure 1. Experimental protocol with stepwise reduction of $\dot{V}_{ECMO}$ and/or Q_{ECMO}.

Figure 2. Schematics for V-A ECMO. $\Delta_{v-ao}CO_2$ is the difference between venous and aortal CO_2 content, $\Delta_{v-LA}CO_2$ is the difference between venous and left atrial CO_2 content, $\Delta_{v-pm}CO_2$ is the difference between venous and post membrane CO_2 content.

Figure 3: Effect of the normalization of the Sweep Gas Flow to Blood Flow Ratio on the V-A ECMO **A**: Scatter plot for Q_{ECMO} vs. $\dot{V}CO_{2ECMO}$. Smallest points represent phase: "*rV_{ECMO}*", middle sized points represent phase "*rQ_{ECMO}"*, large points represent phase: "*$rV\&Q_{ECMO}$"*. No correlations reached significant levels ($p < 0.05$). **B**: Scatter plot for Q_{ECMO} vs. $\dot{V}CO_{2ECMONORM}$, all data points considered. Smallest points represent phase: "*rV_{ECMO}"*, middle sized points represent phase: "*rQ_{ECMO}"* large points represent phase: "*$rV\&Q_{ECMO}$"*. In the phase "*rQ_{ECMO}*", animal 3 did not tolerate the last reduction in V-A ECMO flow.

Figure 4: Correlation between Lung Blood Flow and Carbon Dioxide Elimination at the Lung, absolute values. Scatter plot for Q_{LUNG} vs. $\dot{V}CO_{2LUNG}$, all data points considered. Smallest points represent phase *"rV_{ECMO}"*, middle sized points represent phase: "*rQ_{ECMO}* ", large points represent phase: "*$rV\&Q_{ECMO}$"*. *Note that in animal 1 ventilation and thus $\dot{V}CO_{2Lung}$ is high, because baseline settings at respirator were 5.6l/min (TV 465ml, 12 times / minute). This was the first animal and the ventilator settings were not adjusted from previous settings.* In the phase "*rQ_{ECMO}*", animal 3 did not tolerate the last reduction in V-A ECMO flow.

Figure 5 **A**: Bland Altman plot for all data points during V-A ECMO Weaning. Bias is positive but close to zero with wide limits of agreement. Bias stayed constant over increasing changes in Q_{Lung} ($R^2 = 0.014$). **B**: Scatter plot for the real change in Q_{Lung} vs. the calculated change in Q_{Lung} during V-A ECMO weaning. Smallest points represent phase: "*rV_{ECMO}"*, middle sized points represent phase "*rQ_{ECMO}"*, large points represent phase "*$rV\&Q_{ECMO}$"*. Linear regressions yield : Animal 1: y = 0.75 * x + 73.34, Animal 2: y = 0.44 * x – 47.85, Animal 3: y = 0.73 * x + 7.17, Animal 4: y = 0.8 * x – 30.17. **C**: Scatter plot for subsumed weaning steps for each animals. Linear regressions yield: Animal 1: y = 0.91 * x + 125.05, Animal 2: y = 0.47 * x – 166.98, Animal 3: y = 0.70 * x + 34.8, Animal 4: y = 0.79 * x – 84.95.

Appendix A

Normalization function

1 Formal derivation of a normalized VCO2 for a ventilation/perfusion ratio of one

As $\dot{V}CO2_{ECMO}$ is dependent on the sweep gas flow (17), normalization of the $\dot{V}CO_2$ at any given $\dot{V}/Q$ ratio to a ventilation/perfusion (V/Q) ratio of 1 ($\dot{V}CO_{2ECMONORM}$) will render a variable only dependent on blood flow (Q_{ECMO}) and independent from ventilation (V_{ECMO}). This may facilitate the blood flow prediction in the lung.

The theoretical deduction of this normalization is based on the description of the V/Q ratio as (8):

$$(1)\frac{V}{Q} = \sigma_{CO2} * R * T * (1 + K_c) * \frac{P_{vCO2} - P_{PMCO2}}{P_{PMCO2}}$$

σ_{CO2} is the solubility of CO_2 in blood, R is the gas constant, T is temperature. P_vCO_2 is venous partial pressure and $P_{PM}CO_2$ is the post membrane CO_2 partial pressure. We assume that $P_{PM}CO_2$ is equal to $PeCO_{2ECMO}$, which is measured at the V-A ECMO gas outlet. K_c indicates the equilibration constant of the $CO_2 + H_2O \leftrightarrow HCO3^- + H^+$ reaction at a given pH. It describes the additional liberation of gaseous carbon dioxide from bicarbonate during the passage through the membrane lung. pK is the acid dissociation constant.

$$K_c = \frac{k_1}{k_{-1} * [H^+]}; where \log 10\left(\frac{k_1}{k_{-1}}\right) = -6.1 = pK$$

We assume the following values for BTPS conditions:

$$R = 62.363\frac{(L * mmHg)}{(K * mol)}$$

$$T = 310.5\ Kelvin\ (K)$$

$$K_c = 12$$

$$pH = 7.35$$

$$\sigma_{CO2} = 3.3 * 10^{-5}\frac{Molar}{mmHg}$$

Under the assumption of a constant pH, we can combine these individual constants into one overall constant c.

$$c = \sigma_{CO2} * R * T * (1 + K_c)$$

For the derivation, we assume a constant venous carbon dioxide partial pressure and calculate gas fraction of expired CO_2 ($FeCO_2$).

$$P_{vCO2} = 45\ mmHg$$

$$FeCO_2 = \frac{peCO_{2_{ECMO}}}{bp};\ bp = barometric\ pressure = \ 760\ mmHg$$

We solve eq. 1 for $P_{PM}CO_2$.

$$(2) P_{PMCO2} = peCO_{2_{ECMO}} = c * \ \frac{P_{vCO2}}{(\frac{V}{Q} + c)}$$

A plot of this function shows the known hyperbolic dependency of alveolar, i. e postmembrane pCO_2 from ventilation (V and Q values are assumed from 0 to 4 with an interval of 0.25 l/min).

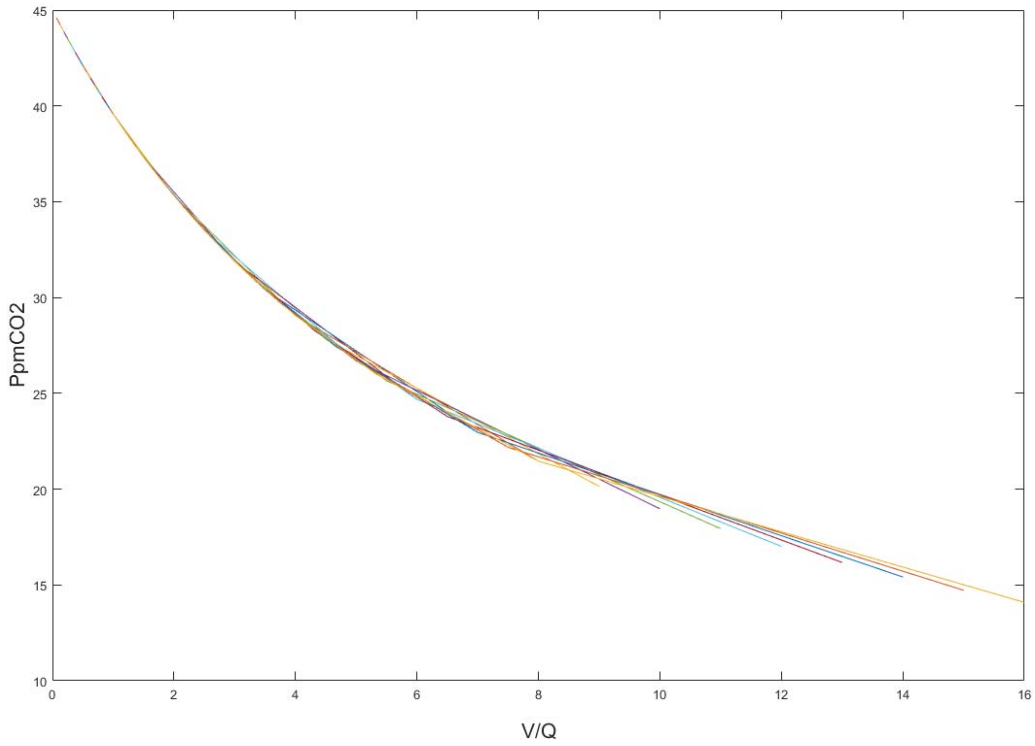

461

462 *Appendix Figure 1. Colors refer to different V/Q data points resulting from the chosen interval of 0.25.*

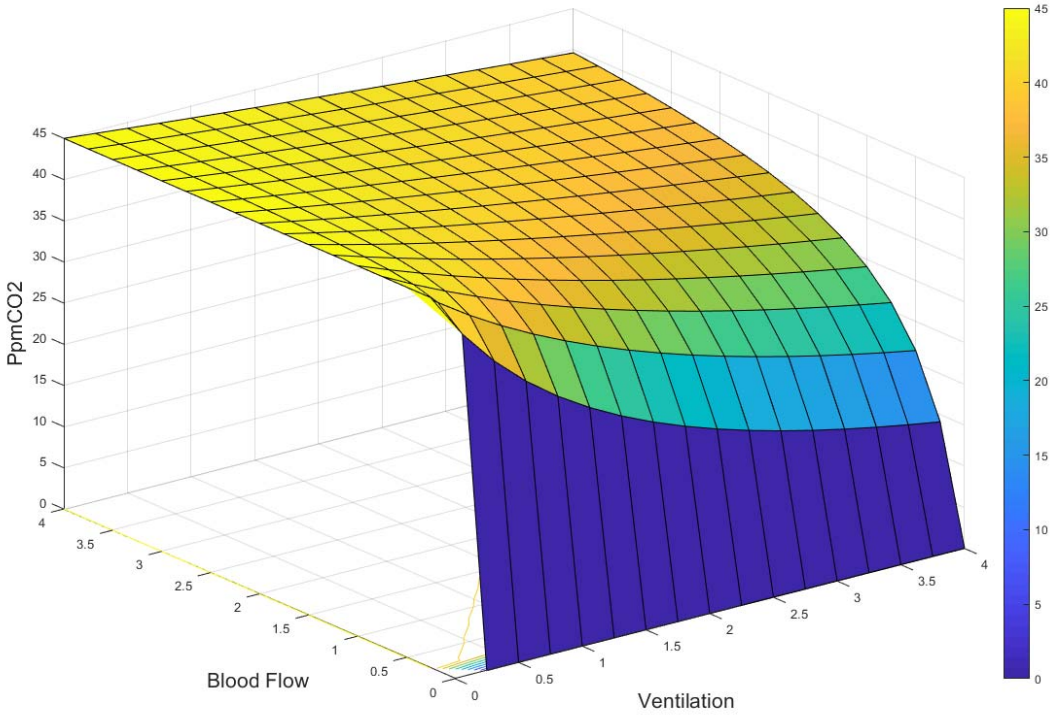

463

Appendix Figure 2

The next step is to calculate $\dot{V}CO_{2ECMO}$ and plot the function (Appendix figure 3). Note, that the factor 1000 is needed to convert the results in ml/min.

$$(3)\ VCO_{2_{ECMO}} = FeCO_2 * V = V * c * \frac{P_{vCO2}}{\left(\frac{V}{Q} + c\right)} * \frac{1000}{760}$$

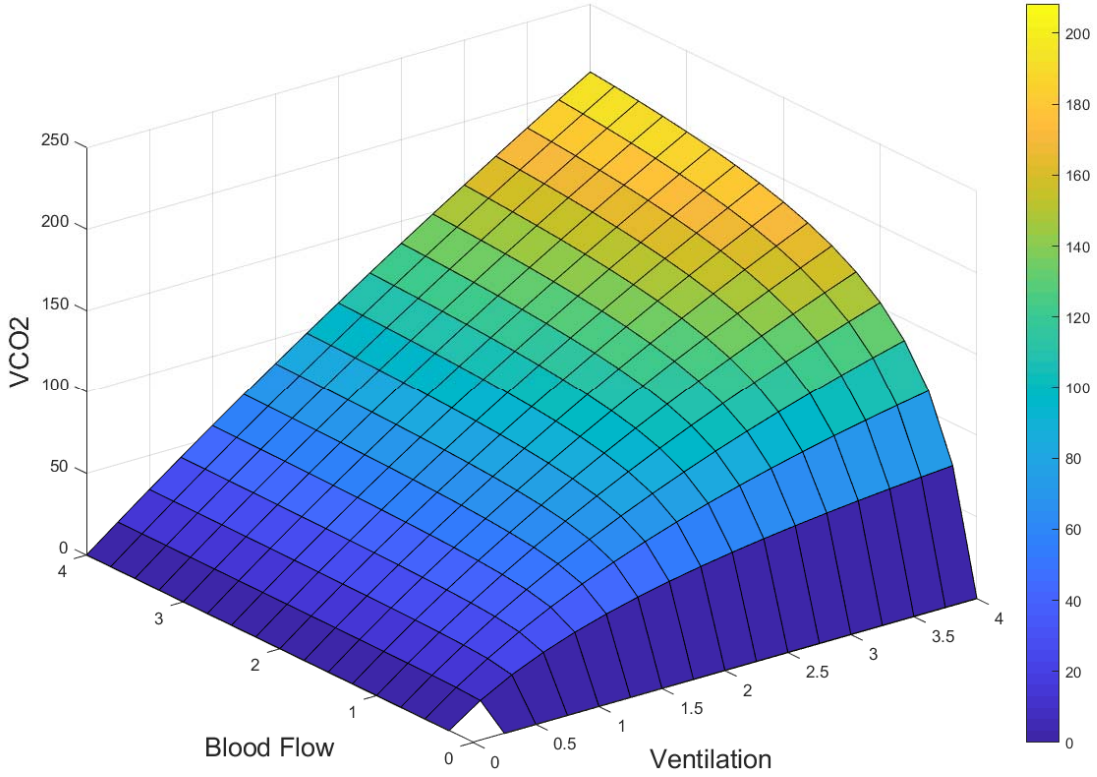

Appendix Figure 3

The diverging effects of the ventilation on the ECMO on PCO_2 and VCO_2 become apparent. In order the represent blood flow, we now normalize the given $\dot{V}CO_2$ to a $\dot{V}$/Q ratio of 1.

We define the correction factor f as the ratio of $\dot{V}CO_2$ at V/Q = 1 to the $\dot{V}CO_2$ at any V/Q. We plot this correction factor f against V/Q.

$$(4)\ f(V,Q) = \frac{\dot{V}CO_2\left(\frac{V}{Q} = 1\right)}{VCO_2}$$

$$f = \frac{V_{\frac{V}{Q}=1} * c * \frac{P_{vCO2}}{(1+c)} * \frac{1000}{760}}{V * c * \frac{P_{vCO2}}{\left(\frac{V}{Q}+c\right)} * \frac{1000}{760}} = \frac{V_{\frac{V}{Q}=1} * \left(\frac{V}{Q}+c\right)}{V * (1+c)}$$

473 As $V_{V/Q=1}$ is equal to Q, we can write:

$$(5)\ f(V,Q) = \frac{Q * \left(\frac{V}{Q}+c\right)}{V * (1+c)} = \frac{\left(\frac{V}{Q}+c\right)}{(1+c)} * \frac{1}{V/Q}$$

474

475 This describes a hyperbolic dependency of f from V/Q scaled with V/Q and c (Appendix figure 4).
476 Note that for a V/Q of 1, the scaling and correction factor is 1.

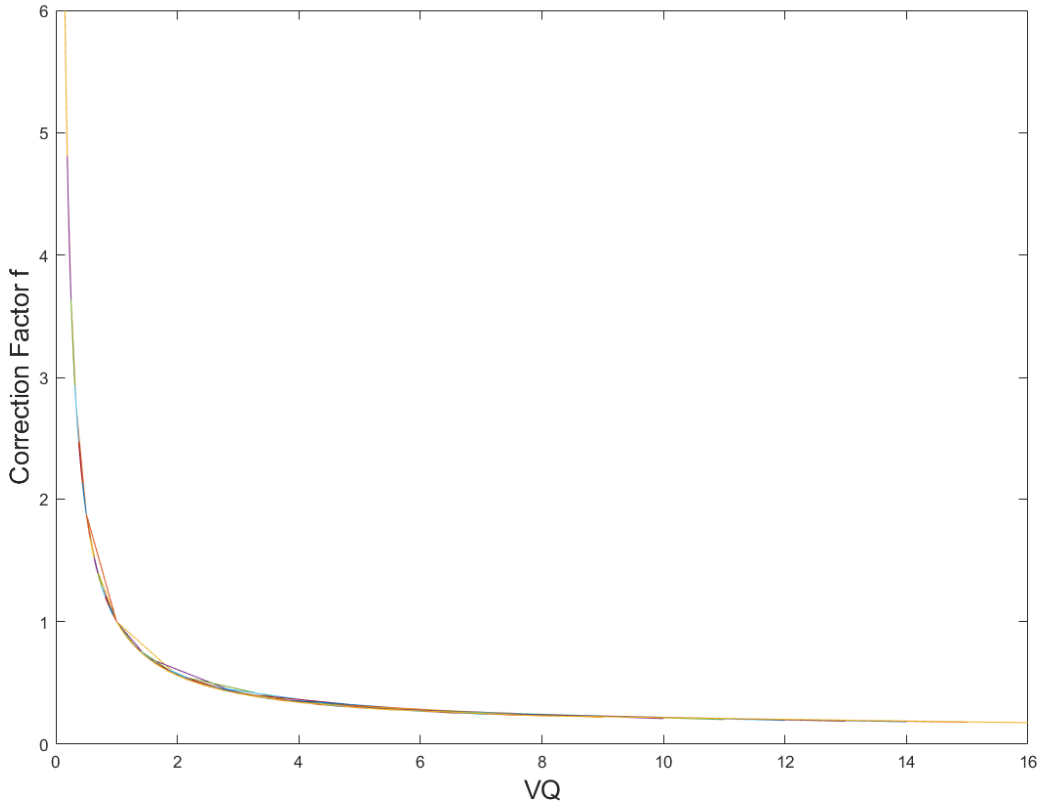

477

478 *Appendix Figure 4: Colors refer to different V/Q data points resulting from the chosen interval of 0.25.*

479 Now, $VCO2_{NORM}$ can be calculated using eq. (3, 5). We plot this new function VCO_{2NORM}, which is
480 independent of V or V/Q (Appendix figure 5).

$$(6)\ \dot{V}CO_{2_{NORM}} = \dot{V}CO_2 * f(V,Q)$$

$$= V * c * \frac{P_{vCO2}}{\left(\frac{V}{Q} + c\right)} * \frac{1000}{760} * \frac{Q * \left(\frac{V}{Q} + c\right)}{V * (1 + c)}$$

$$= Q * c * \frac{P_{vCO2}}{(1 + c)} * \frac{1000}{760}$$

It is clear from this resolved eq. (6), that $\dot{V}CO_{2NORM}$ is dependent on Q and $PvCO_2$, as well as the constant c which itself is dependent on temperature and pH.

It seems intuitive, that this equation (6) can simply be achieved by implementing V/Q = 1 and substituting Q for V in eq. (3). This calculation eliminates the dependency of ventilation and VCO2NORM will represent blood flow at any V/Q (see Appendix figure 5).

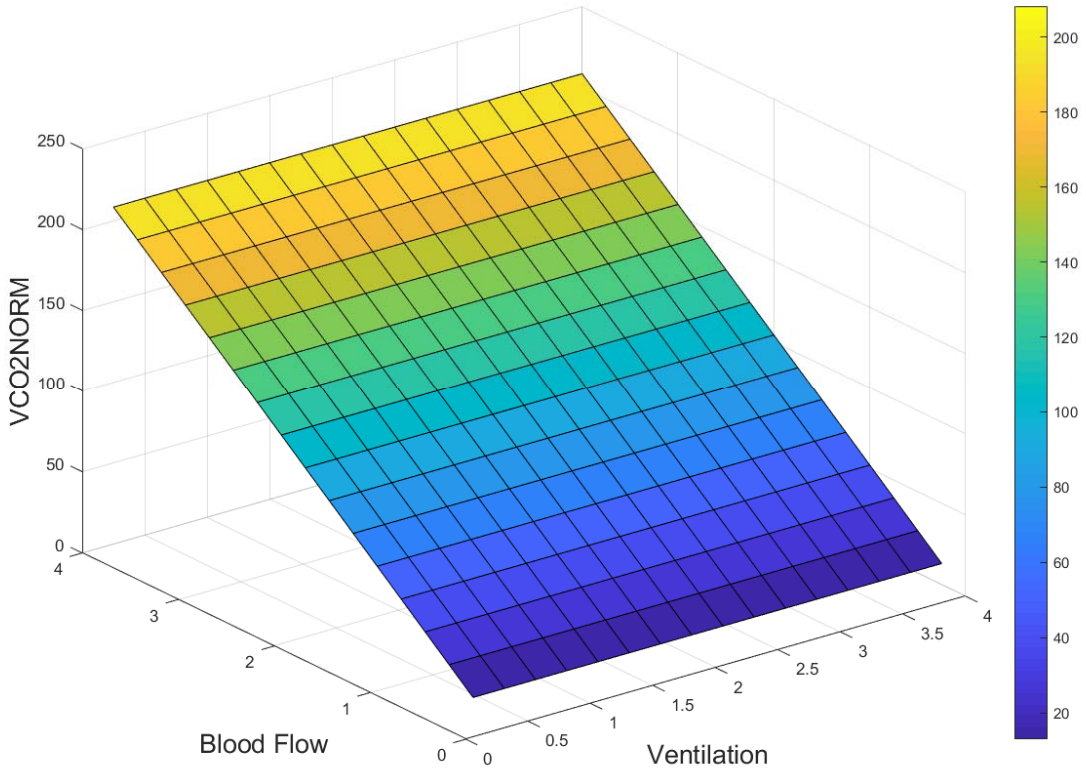

Appendix Figure 5

489 This derivation assumes perfect conditions and depends on venous $pvCO_2$ and pH, which are as
490 a limitation of our study unknown. Therefore, the function has to be approximated from
491 measured data, as described in the following section.

492

2 Retrieving the normalization function from measured Data

We calculated the necessary correction factors using the measured data and eq. 4.

Then, the correction factors were plotted against $\dot{V}/Q$ and the coefficient c was received (Appendix figure 6).

$$(7)\ f(\dot{V}_{ECMO}, Q_{ECMO}) = \frac{Q_{ECMO} * \left(\frac{\dot{V}_{ECMO}}{Q_{ECMO}} + c\right)}{\dot{V}_{ECMO} * (1 + c)};$$

$$c = 1.157;\ 95\%\ CI\ Interval: [1.097, 1.216];\ r^2 = 0.9954$$

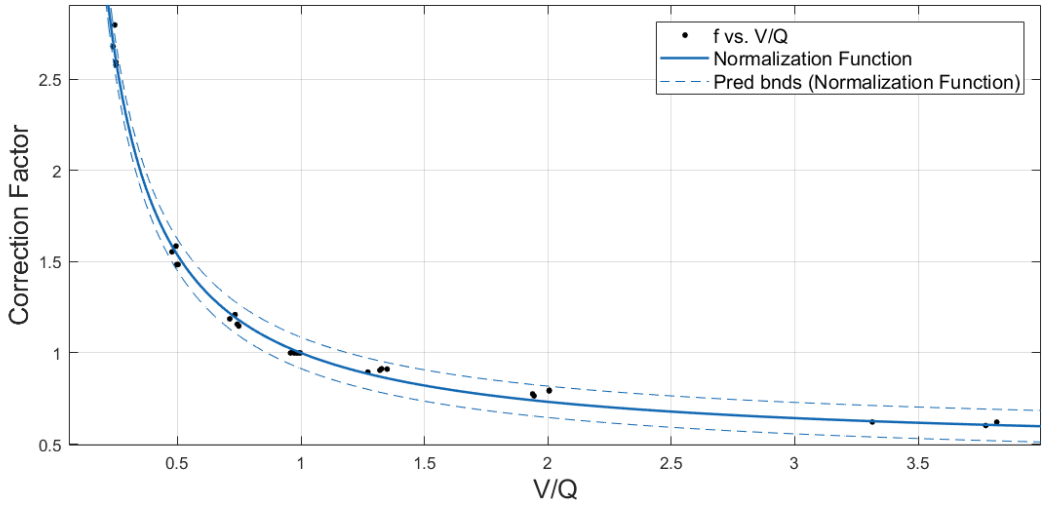

Appendix Figure 6

It is a limitation of our study that our measurements of sweep gas flow (set and read by hand) are much more inaccurate than the blood flow readings. Additionally, instantaneous $PvCO_2$ and pH measurements to calculate c are not available. Inexact ventilation measurements will introduce an error in the position of the normalization curve, where a small shift around a $\dot{V}/Q$ of 1 will have a large impact on the slope of the function. Small errors in measurement of $\dot{V}CO_2$, $\dot{V}$ or Q will therefore largely influence c (Appendix figure 4). However, the calculated function with empirically derived c shows almost perfect goodness of fit and the normalization of $\dot{V}CO_{2ECMO}$ with this correction function shows very strong correlations between $\dot{V}CO_{2ECMONORM}$ and Q_{ECMO} within the range of our measurements (Figure 3, manuscript).

Table 1: Individual data sets

		Animal 1								Animal 2							
		ECMO				Lung				ECMO				Lung			
		V	Q	VCO2	VCO2 norm	V	Q	VCO2	Qcalc	V	Q	VCO2	VCO2 norm	V	Q	VCO2	Qcalc
Step		[ml/min]				[ml/min]				[ml/min]							
V	1	4000	4105	214	217	5600	964	189	3572	4000	4013	222	223	1800	389	52	935
	2	3000	4092	177	212	5600	917	189	3647	3000	4010	194	229	1800	387	61	1077
	3	2000	4049	135	209	5600	1125	195	3778	2000	3982	150	229	1800	370	66	1141
	4	1000	4071	77	203	5600	980	196	3934	1000	3994	86	223	1800	358	60	1065
Q	1	4000	4113	226	229	5600	920	197	3529	4000	4079	259	261	1800	105	64	1006
	2	4000	3147	202	179	5600	1035	200	3520	4000	3016	236	205	1800	503	73	1073
	3	4000	2058	173	128	5600	1458	215	3463	4000	1995	205	150	1800	968	72	966
	4	4000	1207	140	88	5600	1915	244	3348	4000	1048	160	97	1800	1349	87	944
VQ	1	4000	4068	211	213	5600	843	202	3859	4000	4016	245	245	1800	126	75	1236
	2	3000	3231	168	174	5600	1157	199	3686	3000	3008	195	195	1800	560	76	1170
	3	2000	2191	120	126	5600	1376	227	3945	2000	2019	142	143	1800	991	88	1245
	4	1000	1178	66	73	5600	1550	242	3932	1000	1094	67	71	1800	1472	105	1626

		Animal 3								Animal 4							
		ECMO				Lung				ECMO				Lung			
		V	Q	VCO2	VCO2 norm	V	Q	VCO2	Qcalc	V	Q	VCO2	VCO2 norm	V	Q	VCO2	Qcalc
Step		[ml/min]				[ml/min]				[ml/min]				[ml/min]			
V	1	4000	4062	263	266	1800	10	14	217	4000	4170	239	244	2000	59	22	378
	2	3000	4043	228	270	1800	10	18	264	3000	4216	197	240	2000	72	30	528
	3	2000	4025	177	274	1800	5	19	283	2000	4188	154	244	2000	39	34	592
	4	1000	3989	102	266	1800	2	22	333	1000	4186	89	241	2000	21	32	561
Q	1	4000	4031	287	288	1800	4	23	324	4000	4177	248	254	2000	9	31	515
	2	4000	2966	261	225	1800	8	22	296	4000	3031	225	195	2000	294	36	556
	3	4000	1994	228	167	1800	328	42	502	4000	2064	192	142	2000	616	58	845
	4	N/A	N/A	N/A	N/A	N/A	N/A	N/A	N/A	4000	1060	149	91	2000	909	68	801
VQ	1	4000	4074	260	262	1800	9	42	651	4000	4031	231	232	2000	14	49	848
	2	3000	3008	211	211	1800	36	37	529	3000	3098	188	191	2000	259	55	899
	3	2000	1973	168	167	1800	399	57	677	2000	2108	138	142	2000	602	65	964
	4	1000	641	79	64	1800	1327	103	1035	1000	1051	75	78	2000	928	78	1060

Table 1. Individual data for all animals at baseline (step 1 at V, Q, and VQ) and every step of blood flow reduction. ECMO Q and Lung Q denote readings from the respective flow probes, VCO2 values were calculated according to formulas 1 to 3 in the method section using reported barometric pressure for each day (728, 726, 711 and 721 mmHg). Note that 1) in animal 1 ventilation is high because baseline settings at respirator were 5.6l/min (TV 465ml, 12 Freq) and that 2) during phase: “reduction of Q” the cardiovascular system of animal 3 did not support the ECMO Reduction to 25 % of baseline, therefore no measurement is available. VCO2norm refers to a calculated VCO2 for a sweep gas/blood flow ratio normalized towards one (details see Appendix).

Table 2: stepwise reductions

		Animal 1								Animal 2							
		ECMO				Lung				ECMO				Lung			
		ΔV	ΔQ	ΔVCO2	ΔVCO2 norm	ΔV	ΔQ	ΔVCO2	ΔQ Calculated	ΔV	ΔQ	ΔVCO2	ΔVCO2 norm	ΔV	ΔQ	ΔVCO2	ΔQ Calculated
Step		[ml/min]				[ml/min]				[ml/min]				[ml/min]			
V	1 -> 2	-1000	-13	-37	-6	0	-47	0	-1	-1000	-3	-27	6	0	-2	9	-5
	2 -> 3	-1000	-43	-42	-2	0	208	7	122	-1000	-28	-42	1	0	-17	4	-189
	3 -> 4	-1000	22	-59	-7	0	-145	1	-2	-1000	12	-61	-6	0	-13	-6	12
	summed up	-3000	-34	-138	-15	0	16	7	119	-3000	-19	-130	1	0	-32	7	-181
Q	1 -> 2	0	-966	-24	-50	0	115	3	66	0	-1063	-22	-56	0	398	9	160
	2 -> 3	0	-1089	-29	-51	0	423	15	313	0	-1021	-31	-55	0	465	0	-9
	3 -> 4	0	-851	-32	-40	0	457	28	605	0	-947	-44	-53	0	381	15	268
	summed up	0	-2906	-86	-142	0	995	47	984	0	-3031	-98	-164	0	1244	23	419
VQ	1 -> 2	-1000	-837	-43	-38	0	314	-3	-59	-1000	-1008	-50	-50	0	434	0	7
	2 -> 3	-1000	-1040	-47	-48	0	219	28	612	-1000	-989	-52	-52	0	431	12	236
	3 -> 4	-1000	-1013	-54	-54	0	174	15	286	-1000	-925	-75	-72	0	481	17	217
	summed up	-3000	-2890	-144	-140	0	707	41	838	-3000	-2922	-177	-174	0	1346	30	460

		Animal 3								Animal 4							
		ECMO				Lung				ECMO				Lung			
		ΔV	ΔQ	ΔVCO2	ΔVCO2 norm	ΔV	ΔQ	ΔVCO2	ΔQ Calculated	ΔV	ΔQ	ΔVCO2	ΔVCO2 norm	ΔV	ΔQ	ΔVCO2	ΔQ Calculated
Step		[ml/min]				[ml/min]				[ml/min]				[ml/min]			
V	1 -> 2	-1000	-19	-36	4	0	0	3	-15	-1000	46	-42	-4	0	13	8	-84
	2 -> 3	-1000	-18	-50	4	0	-5	2	-8	-1000	-28	-43	4	0	-33	4	-31
	3 -> 4	-1000	-36	-75	-8	0	-3	3	13	-1000	-2	-65	-2	0	-18	-2	-2
	summed up	-3000	-73	-161	0	0	-8	8	-9	-3000	16	-150	-3	0	-38	10	-117
Q	1 -> 2	0	-1065	-25	-63	0	4	-1	-11	0	-1146	-24	-59	0	285	4	88
	2 -> 3	0	-972	-33	-58	0	320	20	326	0	-967	-32	-53	0	322	22	410
	3 -> 4	N/A	N/A	N/A	N/A	N/A	N/A	N/A	N/A	0	-1004	-43	-52	0	293	10	196
	summed up	0	-2037	-59	-121	0	324	19	315	0	-3117	-99	-164	0	900	37	693
VQ	1 -> 2	-1000	-1066	-49	-51	0	27	-5	-99	-1000	-933	-43	-40	0	245	7	158
	2 -> 3	-1000	-1035	-43	-45	0	363	20	459	-1000	-990	-50	-49	0	343	10	195
	3 -> 4	-1000	-1332	-89	-103	0	928	45	588	-1000	-1057	-63	-65	0	326	13	213
	summed up	-3000	-3433	-181	-199	0	1318	61	948	-3000	-2980	-155	-154	0	914	29	565

Table 2. Individual data for all animals for measurements performed at the lung. Note, that during phase: “reduction of Q” the cardiovascular system of animal 3 did not support the ECMO Reduction to 25 % of baseline, therefore no measurement is available.

Figure 1

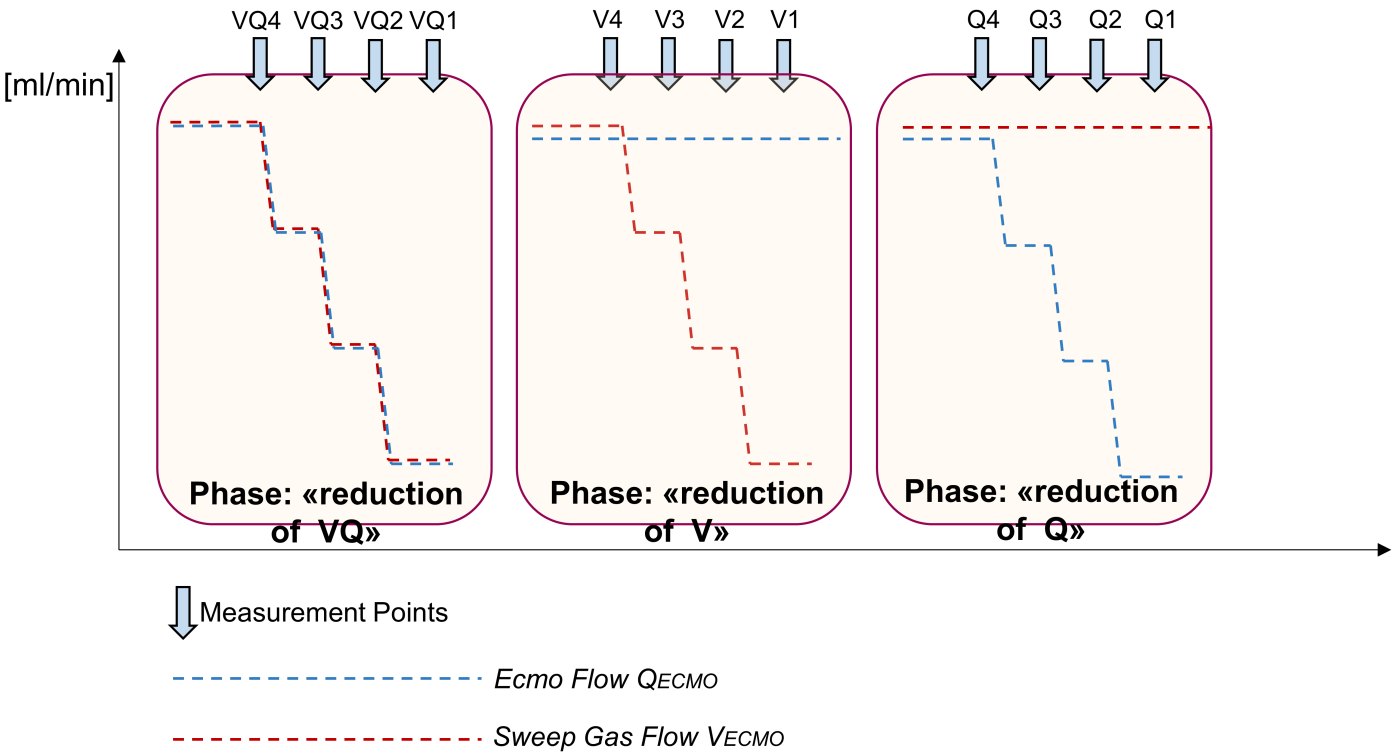

Figure 2

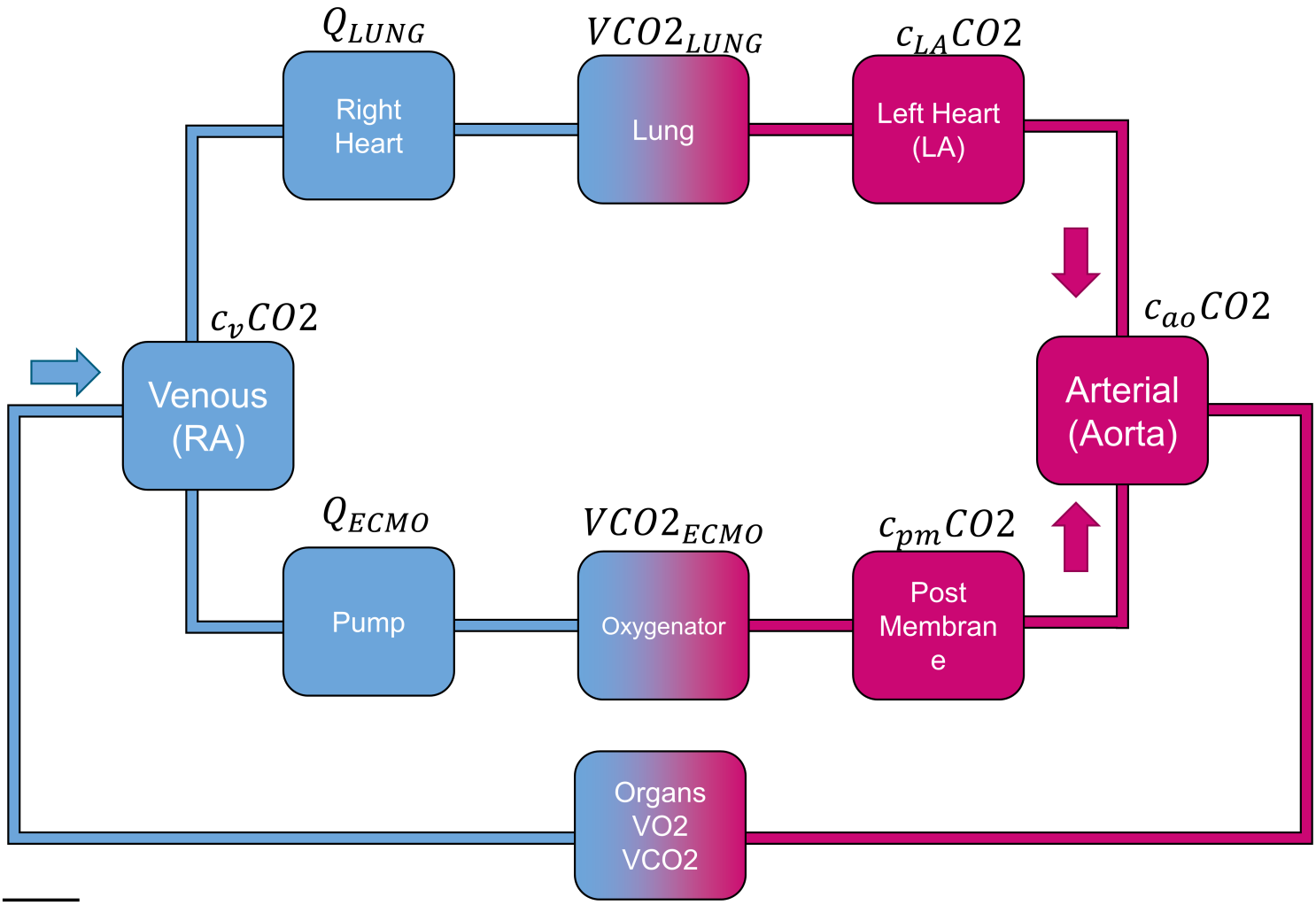

Figure 3A

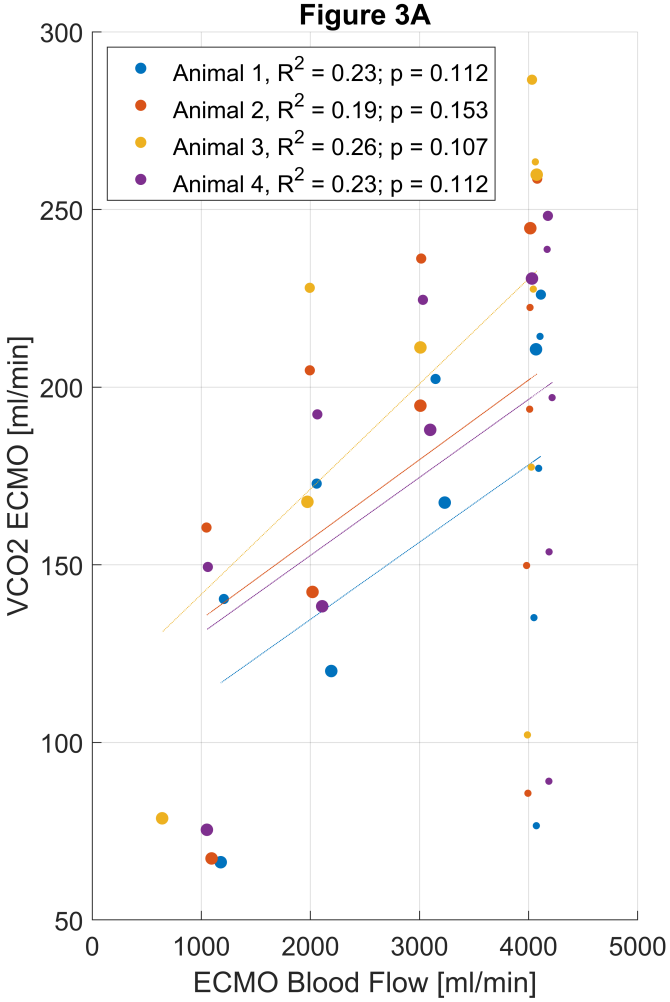

Figure 3B

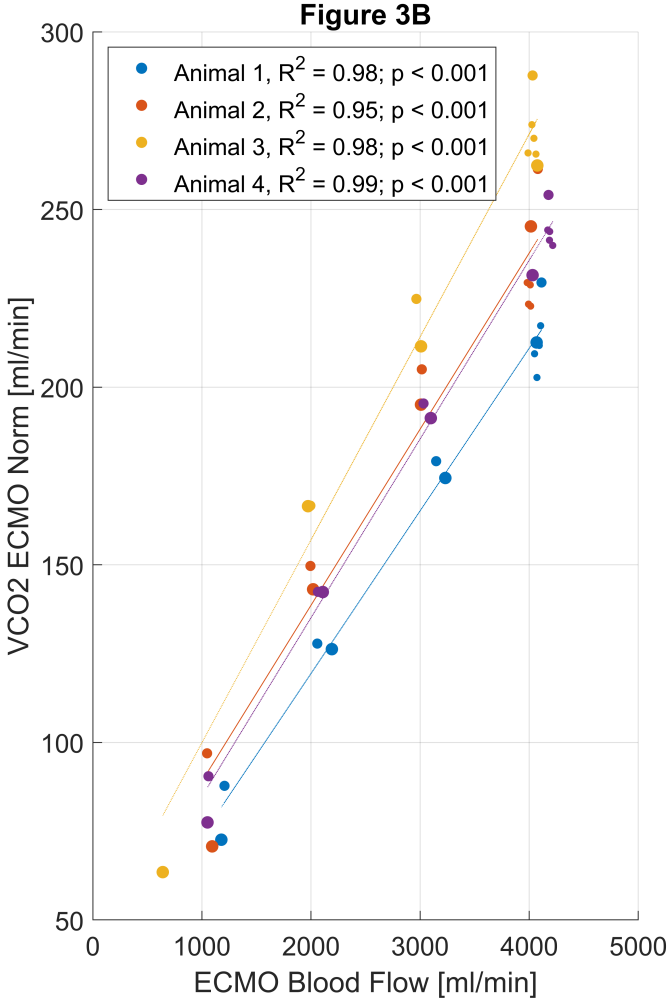

Figure 4

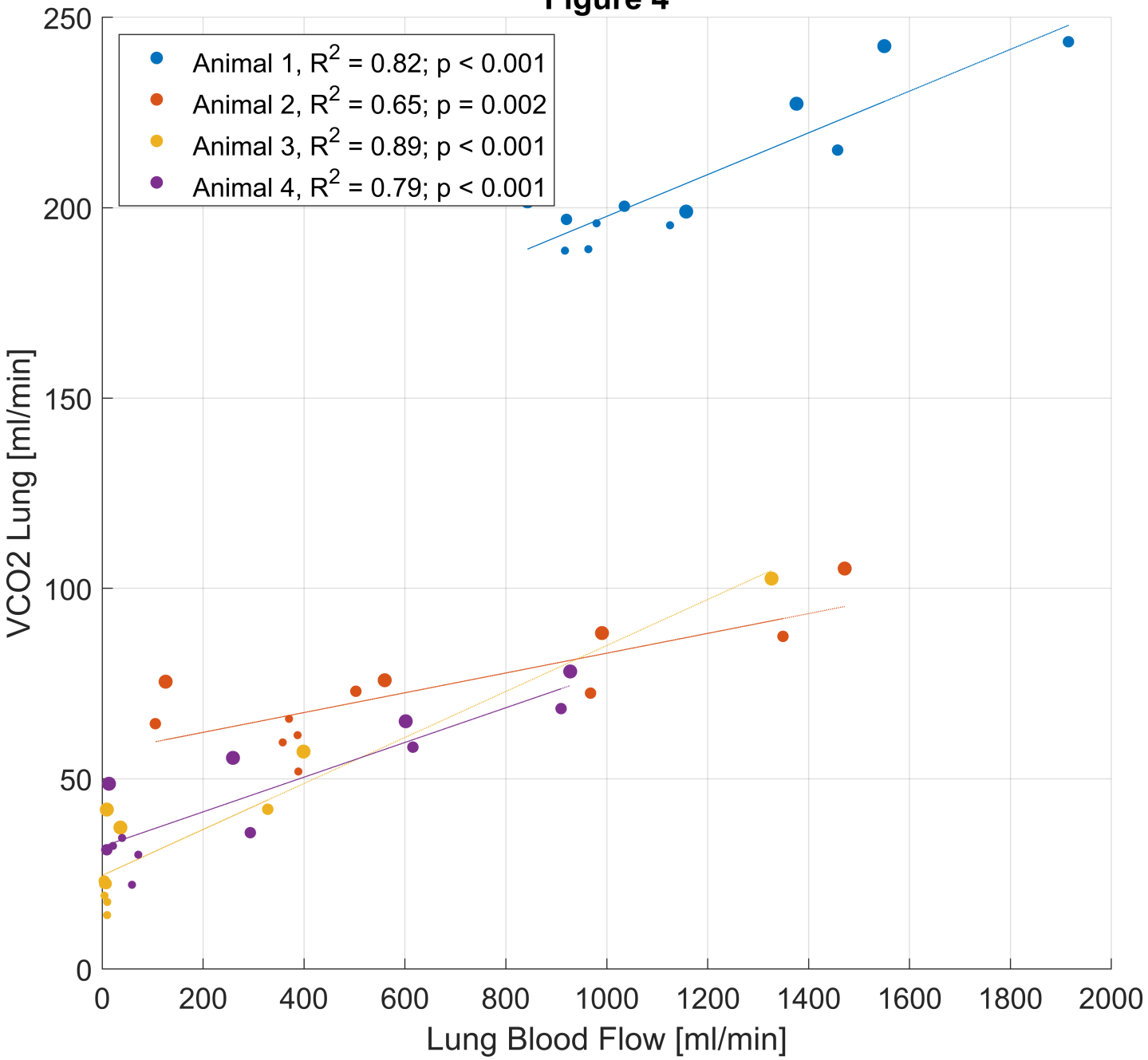

Figure 5A

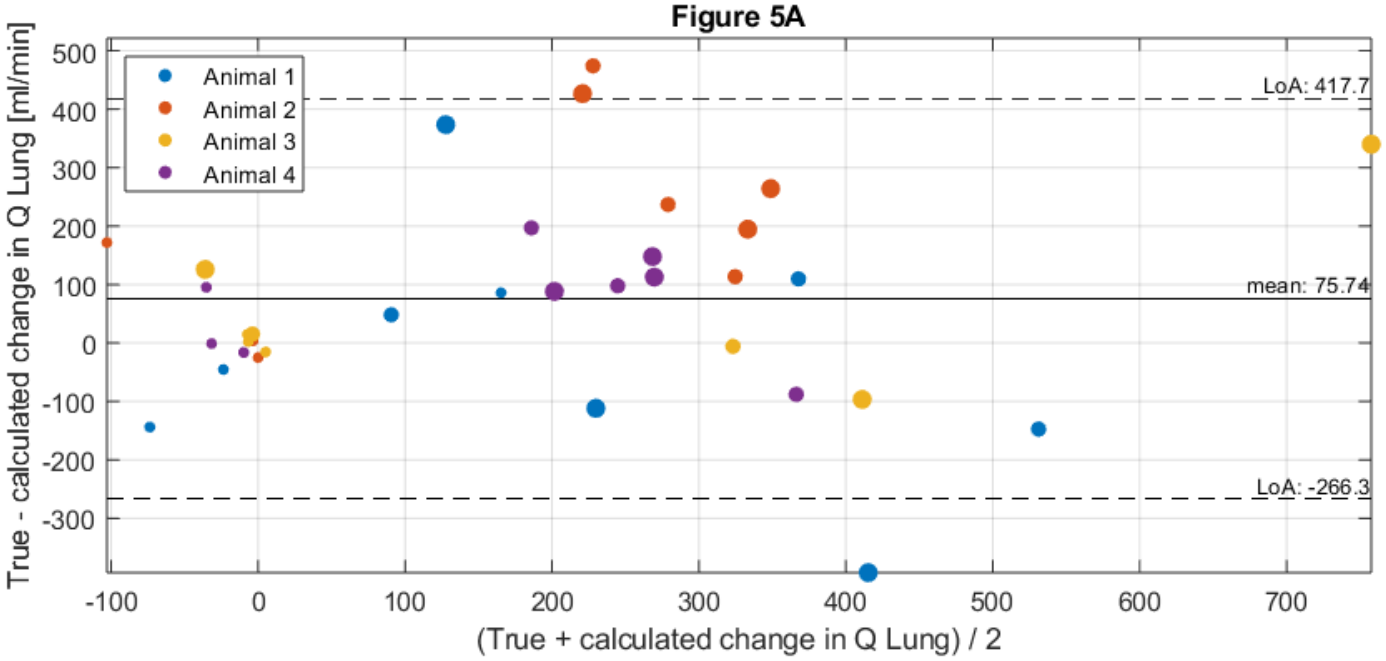

Figure 5B

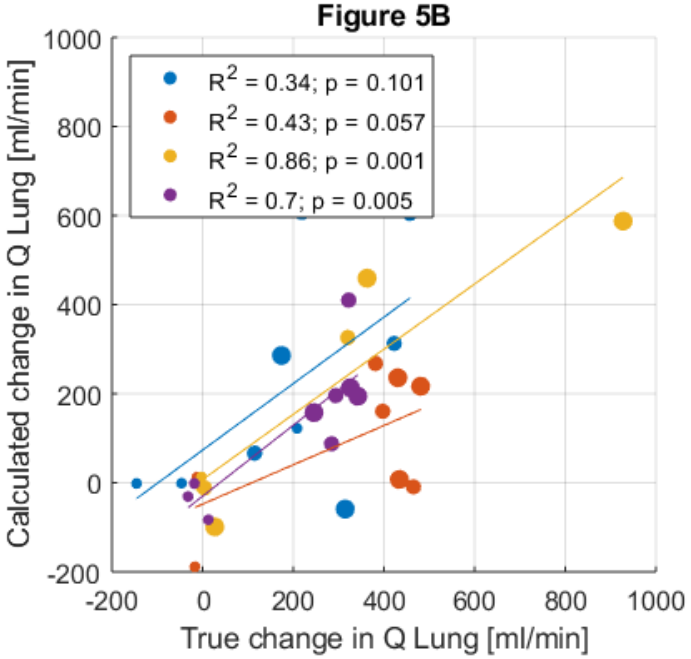

Figure 5C